PEDOSPHERE（土壤圈英文版）

Pedosphere ISSN 1002-0160/CN 32-1315/P doi:10.1016/S1002-0160(19)60837-4

Running title: Impacts of released radionuclides on farmland soil

The distribution of ^{137}Cs and ^{60}Co in plough layer of farmland: evidenced from a lysimeter experiment using undisturbed soil column

Wenxiang Liu[a, #], Hanqing Yu[a, #], Yong Li[a,b *], Surinder Saggar[c], Daozhi Gong[a], Qiong Zhang[d]

[a]*Institute of Environment and Sustainable Development in Agriculture, Chinese Academy of Agricultural Sciences, Beijing 100081, China*

[b]*Guangxi University, Nanning 530005, China*

[c]*Manaaki Whenua – Landcare Research, Private Bag 11052, Palmerston North 4442, New Zealand*

[d]*Nuclear and Radiation Safety Center, Ministry of Environmental Protection of China, Beijing 100082, China*

[*]**Corresponding author:**

Yong Li

Phone: +86-82106016, E-mail: liyong@caas.cn.

[#]These authors contributed equally to this work.

ABSTRACT

Radionuclides fallout during nuclear accidents on the land may impair atmosphere, contaminate farmland soil, crops and even the radionuclides can reach to ground water. Previous researches focused on field distribution of the deposited radionuclides in farmland soils but details of the amounts of radionuclides in the plough layer and the changes in their proportional distribution in the soil profile with time are still inadequate. This study was conducted to determine the vertical migration of ^{137}Cs and ^{60}Co and identify the factors influencing their migration depths in soils. Soil lysimeters representing two farmland soils (Brown and Aeolian sandy soils) growing wheat and maize adjoining Shidaowan nuclear power plant (NPP) in eastern China, were used. At the end of the experiment (day 800), > 96% of added ^{137}Cs and ^{60}Co were retained in the top 0–200 mm soil depth in both soils and very few of ^{137}Cs and ^{60}Co initially migrated to 200–300 mm, but their amounts in this depth increased with time. The migration depth of ^{137}Cs for Aeolian sandy soil was greater than in the Brown soil before day 577, but at the end of the experiment (day 800), ^{137}Cs migrated to the same depth (250 mm) in both soils. Three phases on vertical migration rate of ^{60}Co in Aeolian sandy soil can be identified: an initial rapid movement (0–355 days, v = 219±17 mm year^{-1}), followed by a steady movement (355–577 days, v = 150 ± 24 mm year^{-1}) and a very slow movement (577–800 days, v = 107 ± 7 mm year^{-1}). Whereas its migration rate in Brown soil (v = 133 ± 17 mm year^{-1}) was steady throughout the 800-day period of study. The migration of both ^{137}Cs and ^{60}Co in the two soils appears to be regulated by soil clay and silt fractions providing most of the soil surface area, organic carbon (SOC) and pH, which were manifested on their distribution

coefficient (K_d) of ^{137}Cs and ^{60}Co. The results of this study suggest that most of ^{137}Cs and ^{60}Co remained within upmost layer (0–200 mm depth) in farmland soil following simulated nuclear power plant accident, and few of them reached subsurface (200–300 mm depth). Fixation of radionuclides on to clay minerals may limit their migration in the soil but some of them laterally distribute by soil erosion, uptake by crops and migrate into groundwater in high water table level area after several decades. The remediation measures, therefore, shall focus on reducing their impact on the farmland soil, crop and water.

Key Words: ^{137}Cs; ^{60}Co; Farmland; Migration depth; Brown soil; Aeolian sandy soil

INTRODUCTION

The nuclear power is considered as guaranteed energy supply for economic development in many countries including China, where many nuclear power plants (NPPs) have been constructed in the coastal areas such as Qinshan, Dayawan and Shidaowan. However, in an event of NPP leakage or accident (such as Chernobyl and Fukushima nuclear accidents), large amounts of radionuclides (e.g. ^{137}Cs and ^{60}Co) were released into the atmosphere (Hirose, 2016) and deposited and contaminated the surface soil (Vahabi-Moghaddam and Khoshbinfar, 2012). Most of the fallout radionuclides are adsorbed by clay minerals and some could be taken up by plants from the contaminated soil and join the food chain (Shanthi *et al*., 2012; Teramage *et al*., 2014), causing radioactive contamination. The remaining radionuclides may migrate into the groundwater leading to water pollution (Gupta and Walther, 2014; Fujimura et al., 2015). After the nuclear accidents of Chernobyl and Fukushima, the emergency decontamination practices, including clearing trees and litters (López-Vicente *et al*., 2018), applying wood chips (Cresswell *et al*., 2016), were used to reduce the radioactive contamination. However, residual radionuclides still have impact on agricultural soils and groundwater, and it is necessary to determine the migration dynamics of radionuclides in farmland soil and develop decontamination strategies.

Presently, numerous studies on the migration of radionuclides in soils have already been conducted after various nuclear weapons tests and nuclear accident (Jagercikova *et al.*, 2015). The soil survey in Mediterranean region shows that deposited ^{137}Cs was mainly concentrated at top 120 mm of uncultivated sloping lands while it was concentrated within 0–20 mm soil depth in the forest soil, but the migration can even go deeper in some soils (Gaspar and Navas, 2013; Guillén *et al.*, 2015). Some studies have shown that twenty years after the Chernobyl nuclear accident, the ^{137}Cs migrated into the soil to a depth of 255 mm and in some locations up to 600 mm (Bondarkov *et al.*, 2011). In another experiment, 14 and 26 years after the Chernobyl accident, ^{137}Cs of grassland soil was mainly contained in the surface layer at 40 and 50 mm depths (Bossew *et al.*, 2004; Karadeniz *et al.*, 2015). Similar migration studies have also been conducted in the soil after Fukushima nuclear accident. It was found that two years after the Fukushima nuclear accident, 70% of the ^{137}Cs was contained in the top 50 mm soil depth under forest and grassland land uses, but it had migrated to subsurface (50--100 mm depth) in paddy soil (Takahashi *et al.*, 2015). Research studies also showed that at day 108, 320, 536 and 641 after the Fukushima nuclear accident, ^{137}Cs in farmland migrated to 18, 30, 38 and 45 mm soil depths, respectively (Shiozawa, 2012). Few studies on the migration of ^{60}Co in agricultural soils, a 9 years of lysimeter experiment in Austria found that the vertical migration depth of ^{60}Co

reached at 250 mm soil depth (Shinonaga *et al.*, 2005). Another research on China Loess Plateau (Li *et al*., 2003) reported that most of ^{60}Co migrated to 140 mm soil depth under natural conditions after two years of field investigation. However, detail information on the proportional distribution of radionuclides in farmland was less investigated in the previous studies due to the sampling methodology with larger increment. To obtain specific and accurate characteristics of radionuclides migration, a more detailed sampling is essential.

Generally, fallout radionuclides can bind to solid surfaces by a number of processes that are often classified under the broad term of sorption. The degree of radionuclide sorption on the solid phase is often quantified using the solid-liquid distribution coefficient (K_d), The greater K_d value, the stronger adsorption capacity for the soil with lower migration of radionuclide (Kamei-Ishikawa *et al.*, 2008; Mishra *et al.*, 2015). Soil properties (particle size, organic carbon content, *etc*.) have different impacts on the migration rate of radionuclides (Navas *et al.*, 2002; IAEA, 2010; Dragovi *et al.*, 2012; Sahara *et al.*, 2016). Fine soil particles allow a faster rate of adsorption of radionuclides (Koarashi *et al.*, 2012). Hossain *et al*. (2012) also found that the migration of ^{137}Cs and ^{60}Co in soil with particle sizes ≤ 90 μm was slower than that in relatively coarse textured soil (90 μm–2 mm). In most of the soil types, ^{137}Cs is more readily adhere by clay minerals than large particle mineral due to highly selective reversible adsorption and immobilization processes (Tsukada *et al.*, 2008; Konoplev *et al.*, 2017). Additionally, soil organic matter may play a key role in accelerating the ^{137}Cs fixation process (Dumat *et al*., 1997; Forkapic *et al*., 2017). Many studies found that soil organic carbon and ^{137}Cs have a close relationship because organic matter is a primary and preferential sorbent of ^{137}Cs (Chibowski and Zygmunt, 2002; Staunton *et al*., 2002; Teramage *et al*., 2013; Teramage *et al*., 2016). Wauters *et al*. (1994) reported that humic acid has a positive effect on radionuclides fixation in soils. Hence, it is important to analyses the effects of soil properties on migration of radionuclides in different soils.

From a review of studies on migration of radionuclides described above, it is evident that these researches were focus on distribution of deposited radionuclides in soils by field investigation after nuclear accidents (Mishra *et al.*, 2015; Dowdall *et al.*, 2017), and calculating migration parameters using either analytical or numerical solutions (Bunzl *et al*., 2000; Bossew and Kirchner, 2004). However, the details about amounts of radionuclides at different layers of farmland were lacking in these investigations, and it was not possible to quantitatively determine the proportional distribution of the radionuclides in the soil profile with time. In this study, we monitored the detailed vertical distributions of ^{137}Cs and ^{60}Co in soil profiles using a scraper plate under two types of farmland soils (Brown and Aeolian sandy soils). Our objectives were i) to achieve the characteristics of the temporal changes of ^{137}Cs and ^{60}Co concentration in two farmland soils by lysimeter experiment using undisturbed soil columns and ii) to determine the vertical migration depths of radionuclides in the test soils, and iii) to identify the effects of soil properties on migration of radionuclides in the two soils.

MATERIALS AND METHODS

Study site

The study site is nearby the Shidaowan nuclear power plant (NPP) in Rongcheng county (36 °41'46"–37 °35'14" N, 121 °43'33"–122 °36'12" E), Shandong Province, eastern of China (Fig. 1).

The terrain of study area is tilted from northwest to southeast with an average elevation of 25 m. The climate belongs to warm temperate zone. The annual average temperature is 12℃ and the region receives approximately 2 600 h of sunshine annually. The average annual rainfall is 800 mm. The major soil types are Aeolian sandy and Brown soils distributed within the range of 0–10 km and 10–40 km away from the NPP, respectively. Two sampling sites were selected representing the two soils with altitude of 9 and 68 m, respectively. These sites have grown wheat (*Triticum aestivum L)* and maize (*Zea mays L)* for several decades. The soil was plowed to 250 mm depth and then tilled twice to a depth of 100 mm using rotary cultivator after maize harvest.

Fig. 1 Location of study site (●sampling site).

Collection of undisturbed soil column and background soil samples

Lysimeter experiment was established for farmland soil by plexiglass column. Eight undisturbed soil columns were collected at the typical Aeolian sandy and Brown soils at 9 km and 30 km away from NPP. The plexiglass columns (320 mm diameter × 1 000 mm length, which can reduce wall effect on water and solute transport) with sharp ring in the bottom were used (see Supplementary Fig. S1). These columns were pressed downwards into 300 mm soil depth by hammering. Then soil outside the columns was excavated form a circular pit (400-mm inside diameter, 1 000-mm outside diameter) around the columns to reduce soil compaction during collection. Afterwards, the soil around the columns was scrapped. Columns were then further driven into the soil by repeating hammering, excavation and scrapping steps each time. Finally collecting undisturbed soil column to 700 mm depth. Three 0–700 mm depth cores with 100 mm depth increment were collected using a hand operated core sampler adjoining the undisturbed soil column sampling points which representing background soils. Totally 21 samples (3 cores × 7 depths) were obtained for each soil. The background soil was analyzed for concentrations of the radionuclides and soil properties. The sampling points for undisturbed soil columns were far away from roads and trees to reduce the spatial singularity of soil characteristics. Soil columns and background soil were conducted from 24 March 2014 to 2 April 2014.

Setup of lysimeter experiment

The lysimeter experiment was conducted in soil columns after $^{137}CsCl$ and $^{60}CoCl_2$ solution (pH = 5) was added onto soil surface spread through a pulse for a onetime uniform injection (Supplementary Fig. S2). The total amount of added ^{137}Cs (half-life 30.2 year) and ^{60}Co (half-life 5.3 year) in each column was 300 Bq and 500 Bq, respectively. Tracer solution of ^{137}Cs and ^{60}Co were produced by the China Atomic Energy Research Institute. The experiment was carried out under laboratory-simulated environment consistently with the local meteorological conditions, including rainfall based on 10-year average level (800 mm per year, Supplementary Fig S3), solar radiation (7 hours of irradiation by HPS), etc. To maintain the soil properties and without bacterial growth, the outer wall of soil columns is shaded by black plastic paper. In order to study the temporal changes in the vertical distribution of ^{137}Cs and ^{60}Co in soils, the lysimeter experiment was carried out between February 2015 and April 2017 (duration 800 days) and four observation times were conducted at day

175, 355, 577 and 800 of the experiment, respectively.

Scraper sampling for measurement of migrated radionuclides

To accurately track the vertical migration of radionuclides, a special scraper tool with a sampling area of 706 cm^2 (300 mm diameter) was used to obtain large sample volumes within small depth increments (Takahashi *et al*., 2015). This device used in this study has two components: a metal concentric circular frame place in the soil column, and an adjustable metal scraper that can scrape or remove fixed increments of soil-depth within the frame. Samples were taken with 2 mm increments for the depth at 0–200 mm and 50 mm increments for the depth of 200–700 mm. In order to avoid contamination by the surface soil which can fall down from the wall of the sampling hole, spray glue was used to fix the wall (Kato *et al.*, 2012). Four times soil sampling over 800-day period (175, 355, 577 and 800 days) were carried out for both Brown and Aeolian sandy soils. Two undisturbed soil columns as replicates for each soil type were scraped at each sampling time to obtain ^{137}Cs and ^{60}Co soil samples. During experiment period, the leachate samples from the columns were collected after every simulated irrigation. All leachate samples were used for radionuclides measurement.

Laboratory analysis of soil samples and radionuclides measurements

All soil samples were air dried and sieved pass through 2 mm sieves. The concentrations of ^{137}Cs and ^{60}Co in soil samples and leachate samples were detected by a broad-energy HPGe detector (BE5030, Canberra, USA) with a high relative detection efficiency (50.9%). The detecting system uses a Canberra 747E lead chamber with a 100-mm thickness of the wall and the concentrations of ^{137}Cs and ^{60}Co were analyzed using a DSA 1000 digitizer and a Genie 2000 spectral analysis software. The range of measurable gamma ray energy is 3 keV to 3 MeV and the energy peak of ^{137}Cs and ^{60}Co were 661.6 and 1332.5 keV, respectively. Calibration and quality control of Gamma spectrometer were performed following the protocol of Shakhashiro and Mabit (2009). The spectra were accumulated for 30 000–40 000 s, sufficient to provide an analytical precision of ± 10% for ^{137}Cs and ^{60}Co. The analytical laboratory (CAAS-ALMERA Laboratory) had achieved a high score in radionuclides determination proficiency test organized by IAEA in 2006 (Li *et al.*, 2011).

Soil particle fractions were performed using a laser particle size analyzer (Chappell, 1998). Soil pH was determined with a soil: water solution in 1:2.5 by pH parameter (Page *et al*., 1982). Soil organic matter was determined by the potassium permanganate volumetric method (Soil Science Society of America 2002).

The solid-liquid distribution coefficient (K_d) of radionuclide in soil was determined by static batch method (Relyea, 1982). The soil sample collected from background soil was transferred in to a test tube and centrifuged at 3 000 rpm after adding local groundwater into a test tube, and the supernatant was discarded. After repeated three times, the washing residual liquid weight was recorded according to wet soil weight minus dry soil weight. The soil and added tracer solution with liquid-solid ratio 10:1 were fully mixed in a constant temperature oscillator for 72 h equilibrium time at 25℃ (Kamei-Ishikawa *et al.*, 2008). The supernatant for radionuclides measurements was taken after centrifugation. The solid-liquid distribution coefficient of radionuclide can be expressed as:

$$K_d = \frac{V}{W}\left(\frac{B}{E} - 1\right) - \frac{X}{W}$$

where K_d indicates solid-liquid distribution coefficient of radionuclide (mL g^{-1}), V indicates the tracer volume (mL), W indicates the solid sample weight (g), B indicates the original solution specific activity (Bq mL^{-1}), E indicate the specific activity of the supernatant in the sample tube (Bq mL^{-1}), X indicates the volume (mL) of the solution remaining in soil.

Statistical analysis

The concentrations of added ^{60}Co and ^{137}Cs in soil profiles were calculated by using total concentrations of the radionuclides minus the background values. The soil depth was defined as migration depth of radionuclide when the mean concentration was more than 2σ (twice the standard deviation of the measured values) at a fore-mentioned depth. The migration rate of ^{137}Cs and ^{60}Co in soil was calculated by their migration depth divided by the observation time.

The distribution curves of added radionuclides in the soil profile were fitted using exponential model by the software Sigmaplot 12.5. Differences of soil properties and K_d values between different soils were done by one-way analysis of variance (ANOVA) through a statistical software SPSS 19.0.

RESULTS

Background concentrations of ^{137}Cs and ^{60}Co in the soil profiles

Fig. 2 is the concentration of background ^{137}Cs in two soil types. The maximum concentration of background ^{137}Cs in Brown and Aeolian sandy soils was 2.5 ± 0.2 Bq kg^{-1} and 1.6 ± 0.1 Bq kg^{-1}, respectively. Background ^{137}Cs was present mainly in surface soil (0–300 mm depth) and it decreased with increasing soil depth. The mean total background ^{137}Cs was 124 Bq in lysimeters containing Brown soil and 67 Bq in the lysimeters containing Aeolian sandy soil. No background ^{60}Co was detected in these two soils.

Fig. 2 Background concentration of ^{137}Cs in Brown and Aeolian sandy soils. Each value represents the mean of three replicates ± standard error shown by horizontal bars.

Dynamics change of added ^{137}Cs and ^{60}Co concentrations in soil profiles

The concentrations of ^{137}Cs and ^{60}Co in the top layer (0–2 mm soil depth) during observation period were the highest exceeding 100 Bq kg^{-1} in both Brown and Aeolian sandy soils (Figs. 3 and 4). In the soil profiles, the amounts of ^{137}Cs and ^{60}Co decreased with increasing soil depth, while the concentration of ^{137}Cs and ^{60}Co in deep depth increased with time. Except the surface layer (0–2 mm soil depth), the concentration of ^{137}Cs and ^{60}Co at other depths of Aeolian sandy soil was higher than those of Brown soil. No ^{137}Cs and ^{60}Co were detected in the leachate samples from both soils during 800-day period of this experiment.

Fig. 3 Dynamic migration of the added ^{137}Cs in soil profiles. Each value represents the mean of ^{137}Cs concentration in two undisturbed soil columns ± standard error shown by horizontal bars.

Fig. 4 Dynamic migration of the added ^{60}Co in soil profiles. Each value represents the mean of ^{60}Co concentration in two undisturbed soil columns ± standard error shown by horizontal bars.

Periodic migration depth of added ^{137}Cs and ^{60}Co in test soils

The migration depth of ^{137}Cs in both soils during experiment period was increased from 52 mm to 250 mm from 175th day to 800th day (Fig. 5). In Aeolian sandy soil, it migrated 10%–46% deeper than in Brown soil till 577th day but reached the same depth (250 mm) at 800th day in both soils. The proportion of ^{137}Cs to total input decreased in Brown soil and Aeolian sandy soil from 95% to 80% and from 97% to 88%, respectively, at 0–100 mm soil depth with time increase. Only < 2% of ^{137}Cs was migrated to 200–300 mm depth in both soils at the end of observation time (Table I).

Fig. 5 Variation in migration depths of ^{137}Cs and ^{60}Co in Brown and Aeolian sandy soils during 800-day observation. Each value represents the mean of migration depth of ^{137}Cs and ^{60}Co in two undisturbed soil columns ± standard error shown by vertical bars.

TABLE I

Percentage (%) of ^{137}Cs and ^{60}Co to total input distributed in each depth of Brown and Aeolian soils measured periodically during 800-day study

Soil type	Days	Soil depth（mm）					
		^{137}Cs			^{60}Co		
		0--100	100--200	200--300	0--100	100--200	200--300
Brown soil	175	95.04±0.22	4.96±0.20	no.	96.84±1.62	3.16±1.57	no.
	355	94.88±0.68	5.12±0.71	no.	94.65±1.56	5.35±1.33	no.
	577	85.55±0.60	13.59±0.17	0.86±0.05	87.57±0.45	11.27±0.61	1.16±0.37
	800	80.15±0.24	18.53±0.25	1.32±0.46	80.67±2.31	16.19±2.95	3.14±0.56
Aeolian sandy soil	175	96.84±2.26	3.16±0.55	no.	99.98±0.36	0.02±0.34	no.
	355	94.64±3.08	5.36±3.05	no.	94.80±5.55	5.20±5.81	no.
	577	91.34±1.84	8.00±1.59	0.66±0.04	91.76±1.60	7.54±0.38	0.70±0.06
	800	88.16±1.57	9.88±1.48	1.96±0.01	88.67±0.60	9.32±0.60	2.01±0.04

Each value represents the mean of three replicates ± standard error; ND = Not detectable.

The migration depth of ^{60}Co in soil changed from 81 mm to 300 mm from 175th day to 800th day. The migration change of ^{60}Co in Aeolian sandy soil occurred in three phases: an initial rapid movement (0–355 days), followed by a steady movement (355–577 days) and very little migration (577--800 days). The migration rate of ^{60}Co in the Brown soil was steady throughout the 800–day period of study. At the end of experiment (800-day), the amount of ^{60}Co in Brown soil and Aeolian sandy soil surface (0–100 mm) was 80.67% ± 2.31% and 88.67% ± 0.60%, respectively (Table I). Similarly, the proportion of ^{60}Co to total input decreased in Brown soil and Aeolian sandy soil from

97% to 81% and 99% to 89%, respectively, at 0–100 mm soil depth with time increase. About 3% of ^{60}Co was migrated to 200– 300 mm depth in both soils at the end of observation time.

Potential impact of soil properties on migration of radionuclides in soils

Both soils had similar bulk density and texture [low clay (2%–5%) and sand (13%–15%) contents and high silt (80%–83%) content] (Table II). Soil organic carbon (SOC) was between 3.9 to 12.1 g C kg^{-1} in Brown soil and 0.3 to 11.0 g C kg^{-1} in Aeolian sandy soil. The Brown soil was more acidic (pH; 4.90 to 6.49), than Aeolian sandy soil (pH; 5.88 and 7.54). The soil electrical conductivity (EC) significantly reduced with depth for both soils ($P < 0.05$) and the EC of Brown soil was higher than that of Aeolian sandy soil. The K_d values show that K_d (^{137}Cs) is much higher than K_d (^{60}Co) (Table III). There was no significant difference in K_d within 0–300 mm soil depth for the two soil types while it decreased significantly with depth below 300 mm soil depth ($P < 0.05$), aside from K_d (^{137}Cs) at 500-600 mm soil depth.

TABLE II

Physical and chemical properties of Brown and Aeolian sandy soils

Soil type	Depth (mm)	Bulk density (g cm^{-3})	Particle size distribution (%)			SOC (g kg^{-1})	pH	EC (µs cm^{-1})
			Sand	Silt	Clay			
Brown soil	0-100	1.45 ±0.04c A*	13.36 ±3.71a bA	83.85 ±4.76a A	2.79 ±1.09a A	20.87 ±1.49a A	4.90 ±0.04b A	109.11 ±13.56a A
	100-200	1.50 ±0.02b cA	14.53 ±1.61a bA	83.42 ±1.54a A	2.05 ±0.39a B	17.58 ±0.75 bB	4.94 ±0.08b A	103.66 ±11.03a bA
	200-300	1.56 ±0.04b A	14.86 ±0.60a bA	83.08 ±0.70a A	2.06 ±1.19a A	12.89 ±0.63c B	5.00 ±0.12b A	87.12 ±7.06bA
	300-400	1.67 ±0.06a A	14.24 ±1.78a bB	81.17 ±2.94a A	4.59 ±3.59a A	11.31 ±0.43 dA	5.26 ±0.19a A	83.88 ±8.78bA
	400-500	1.62 ±0.02a bA	11.16 ±2.37b B	85.72 ±2.50a A	3.12 ±1.45a A	9.38 ±0.90e A	5.64 ±0.36a A	84.54 ±12.21bA
	500-600	1.62 ±0.03a bA	13.09 ±2.43a bB	84.64 ±3.66a A	2.27 ±1.34a A	7.58 ±0.48f A	6.15 ±0.17a A	61.79 ±7.22cA
	600-700	1.68 ±0.08a A	15.96 ±2.98a A	81.45 ±2.62a A	2.59 ±0.78a B	6.73 ±0.28g A	6.49 ±0.20a A	61.05 ±7.08cA
Aeolian sandy soil	0-100	1.47 ±0.07c A	14.88 ±3.57a A	81.81 ±1.34a A	3.31 ±2.48b A	19.02 ±0.90a B	5.88 ±0.19a A	75.43 ±13.81aB
	100-200	1.48 ±0.04b cA	15.51 ±4.11b A	80.88 ±4.57a A	3.61 ±0.75b A	18.64 ±1.36 bA	6.06 ±0.23a A	68.96 ±10.22bB
	200-300	1.59 ±0.08b A	13.84 ±1.83a A	83.84 ±1.76a A	2.32 ±0.26b A	13.61 ±0.90c A	6.84 ±0.15a B	52.89 ±5.06bB
	300-400	1.57 ±0.03b	21.33 ±1.78a	75.46 ±2.94b	3.22 ±3.59b	11.57 ±1.08	7.14 ±0.12a	61.47 ±10.90bB

0	A	A	A	A	dA	A	
400-50	1.59±0.05b	18.97±2.37a	75.68±2.37b	5.36±1.45b	8.18±1.07e	7.29±0.11a	57.55±7.64bB
0	A	A	B	A	B	A	
500-60	1.64±0.02b	18.80±2.43a	78.14±3.66a	3.06±1.34b	6.94±0.54f	7.46±0.09a	56.11±7.79bB
0	A	A	bA	A	B	A	
600-70	1.77±0.07a	18.52±2.35a	75.92±2.07b	5.56±1.59a	5.14±0.55g	7.54±0.09a	65.95±6.60bA
0	A	bA	B	A	B	B	

*Means ± standard deviations in the same column with the same small letters under the same soil type are not significantly different among treatments at $P < 0.05$ probability level. Means in the same column with the same capital letters under the same soil type are not significantly different between same depths at $P < 0.05$ probability level.

TABLE III

The solid-liquid distribution coefficient (K_d) of ^{137}Cs and ^{60}Co for Brown and Aeolian sandy soils

Depth (mm)	K_d (^{137}Cs) (ml g^{-1})		K_d (^{60}Co) (ml g^{-1})	
	Brown soil	Aeolian sandy soil	Brown soil	Aeolian sandy soil
0-100	1303±51aA*	1237±99bA	950±46bA	720±41bB
100-200	1626±58aA	1515±92aA	1079±54aA	1028±39aA
200-300	1059±57cA	1121±75bA	904±52bA	578±99cB
300-400	712±65eB	943±31cA	579±14cA	509±79cA
400-500	662±16eA	513±29dB	387±70dA	406±15dA
500-600	882±34dA	539±81dB	260±38eA	281±60eA
600-700	400±17fA	284±14eB	223±29eA	230±15eA

*Means ± standard deviations in the same column with the same small letters under the same soil type are not significantly different among treatments at $P < 0.05$ probability level. Means in the same row with the same capital letters under different soil type are not significantly different between same depth at $P < 0.05$ probability level.

DISCUSSION

Migration depths of ^{137}Cs and ^{60}Co in farmlands

Our results found that the maximum migration depth of ^{137}Cs and ^{60}Co were no more than plough layer (250–300 mm), and most of them were constrained at surface soil (0--100 mm) in Brown and Aeolian soils at day 800 of the experiment (Table I). Takahashi *et al.* (2015) reported that the migration depth of ^{137}Cs in agricultural soil with high bulk density increased with time and varied from 18 mm to 45 mm at day 108 and day 641 after the Fukushima nuclear accident. ^{137}Cs migrated in the cultivated red soil of Poland and Sweden to 255 mm soil depth after twenty years of the Chernobyl nuclear accident (Bondarkov *et al.*, 2011). The variation of the migration depth in our study was consistent with previous researches that high activity concentration of ^{137}Cs was constrained at the surface layer of farmland near Fukushima power plant (Nakano and Yong, 2013; Shiozawa, 2012). The limited studies on the migration of ^{60}Co in agricultural soils found that the vertical migration of ^{60}Co accumulated in top layer (0–200 mm) and only about 3% of the added ^{60}Co

or even smaller was reached in the deeper soil layers (200–250 mm) after 9 years of lysimeter experiment (Shinonaga *et al.*, 2005). Another research on China Loess Plateau (Li et al., 2003) reported that most of ^{60}Co was retarded in surface loess, while few of ^{60}Co has migrated to 100 mm depth in loess under natural conditions after two years of field investigation. The migration depth of ^{60}Co in our study was consistent with these researches that few of ^{60}Co can be reached deeper soil depth (200–300 mm).

The variations of migration depths of ^{137}Cs and ^{60}Co in different studies are closely related to soil types, experiment methods and meteorological conditions (Bondarkov *et al.*, 2011; Nakano and Yong, 2013; Li *et al.*, 2003; Shinonaga *et al.*, 2005; Shiozawa, 2012; Takahashi *et al.*, 2015). The migration rates of ^{137}Cs and ^{60}Co (v = 107–133 mm year^{-1}) in our study were higher than in farmland and paddy field near the FDNPP (v = 40–50 mm year^{-1}) due to lower clay content in our test soils than in the agricultural soil near the FDNPP (Takahashi *et al.*, 2015). In addition, unlike field investigation near the FDNPP, our lysimeter experiment was conducted in the laboratory under simulated weather condition, which resulted in higher migration rate in our study for avoiding extreme climate events to disturb experiment conduction. Different meteorological conditions also can cause different migration rates of radionuclides in soils. For example, a high evapotranspiration (1830 mm per year) and less rainfall (390 mm per year) in loess of North China (Li *et al.*, 2003) can result in upwards transportation of ^{137}Cs and ^{60}Co (Shinonaga *et al.*, 2005).

Direct and in-direct influencing factors on migration of ^{137}Cs and ^{60}Co in farmland soils

Our results found that ^{137}Cs and ^{60}Co in Aeolian sandy soil were migrated faster than in Brown soil before day 577 (0–200 mm soil depth). However, the migration rates of ^{137}Cs and ^{60}Co in Aeolian sandy soil slower than in Brown soil at the end of experiment (200–300 mm soil depth) (Fig. 5). Soil properties including soil particle size fractions, SOC, pH, K_d, have direct impacts on vertical distribution of radionuclides in soils (IAEA, 2010; Sahara *et al.*, 2016). To assess the effect of soil properties on migration of radionuclides in the two soils, the ratio of clay+silt fraction, SOC, pH, K_d and radionuclide migration depth (D) in Aeolian sandy soil to Brown soil was used as an indicator (Fig. 6). D (^{137}Cs) and D (^{60}Co) before 577 days of the experiment (0–200 mm soil depth) was larger than 1, and while it decreased with time (< 1) between day 577 and 800 of the experiment (200–300 mm soil depth). Radionuclides can be adhered more readily by fine fractions (clay and silt sized) of soils, due to larger surface area resulting in highly selective reversible adsorption and immobilization processes (Tsukada *et al.*, 2008; Koarashi *et al.*, 2012; Konoplev *et al.*, 2017). In addition, soil organic matter, particularly of simple organic acids and fulvic and humic acids of low molecular weight, contains functional groups that can form complexes with radionuclides in the soil profile (Dragovi *et al.*, 2012), and affect the vertical distribution of radionuclides in soils (Koarashi *et al.*, 2012). Soil particle size fraction can also reflect the magnitude of saturated and non–saturated hydraulic conductivity (Pachepsky and Park, 2015). It was reported that saturated hydraulic conductivity is negatively correlated with soil clay content, but positively correlated with ^{137}Cs specific activity in soil (Dragovi *et al.*, 2012). Our results were consistent with these findings that the ^{137}Cs and ^{60}Co in soil solution can penetrated faster in 0–200 mm depth of Aeolian sandy soil than that of Brown soil due to lower silt fraction (with large proportion of soil particle size) and SOC content in Aeolian sandy soil than in Brown soil. Similarly, the radionuclides infiltrated faster in 200–300 mm depth of Brown soil than that of Aeolian sandy soil due to higher silt and SOC content in latter soil depth.

Fig. 6 The ratio of clay+silt fraction, SOC, pH, K_d, migration depth (D) of radionuclides (^{137}Cs and ^{60}Co) in Aeolian sandy soil to in Brown soil at each sampling time.

The ratio of pH also increased with time and it was larger than 1 after 577 days of the experiment (Fig. 6), suggesting that the pH at 200–300 depth of Aeolian sandy soil was higher than in Brown soil which make more ^{137}Cs and ^{60}Co became immovable. The reason is that higher pH in test soil will regulate the affinity and activity of radionuclides by increasing the amount of negative charge on surface edges of the clay for variable–charged clay types (van der Graaf *et al.*, 2007; Sahara *et al.*, 2016), which resulting in competitive adsorption in clay minerals between radionuclides and ions.

It is also supported by the ratio of K_d (^{137}Cs) and K_d (^{60}Co) which increased with time during the observation period of experiment, indicating more ^{137}Cs and ^{60}Co were absorbed at 200–300 mm depth of Aeolian sandy soil than that of Brown soil. That means ^{137}Cs and ^{60}Co migrated faster in Brown soil than in Aeolian sandy soil after 577 days of experiment (200–300 mm soil depth).

Additionally, agricultural management practices, such as tillage and fertilization, affect soil properties (Šimanský *et al.*, 2019), thereby these practices have in-direct impacts on migration of ^{137}Cs and ^{60}Co in farmland soils. Tillage has an impact on the ability of the soil to adsorb and retain water and solute, and it depends on the level of soil disturbance (Alvarez and Steinbach, 2009; Blanco-Canqui *et al.*, 2017). Tillage would increase water infiltration by disrupting compacted layers and loosening soil bulk density relative to no-till management (Salem *et al.*, 2015). It also may cause redistribution of deposited radionuclides in farmland soil after NPP accident resulting from soil mixing by plowing (Takahashi *et al.*, 2015). Fertilization can increase straw residue and root biomass input into soil systems, eventually causing an increase in the SOC content and soil aggregation (Tian *et al*., 2015). In our study, soil properties were homogenous in plough layer due to mixture by frequent and intensive agricultural management practices with a long-term history growing *wheat and maize*. Long–term tillage and fertilization on the agricultural soils resulted in uniform soil properties and lead to similar migration rates of radionuclides in soil plough layers.

Implication of released ^{137}Cs and ^{60}Co on surface water, plants and groundwater

The results of this study indicated that most of ^{137}Cs and ^{60}Co predominantly bound to fine particles at top layer (0–100 mm) of farmland (Fig.3 and 4). After fixation in surface soil, heavy rainfall and flood events induced water erosion would transfer radionuclides to low-lying area through lateral redistribution (Lepage *et al.*, 2016), and subsequently move to the surface water system (Yoshimura *et al.*, 2015). In addition, during strong wind events, significant volumes of contaminated sediments are transported downstream by wind erosion (Evrard *et al.*, 2013).

The released radionuclides not only impact surface water, but also have threats to farmland system. Our results suggested that ^{137}Cs and ^{60}Co were almost entirely distributed in the plough layer of farmland at the end of the experiment. The plough layer is rich in nutrients and some of radionuclides may be absorbed by roots and accumulate in plants when the crop roots uptake nutrients from the soil (Shanthi *et al.*, 2012). Crops enriched in radionuclides can cause food contamination and endanger human health (Walther and Gupta, 2015). Various crops with different absorptive capacities and transfer factors are often used as plant remediation. The study reported that transfer factors of

^{137}Cs and ^{60}Co to wheat were 0.021 ± 0.027 in stems and 0.009 ± 0.012 in grains, to maize were 0.041 ± 0.066 in stems and 0.005 ± 0.013 in grains (Gerzabek *et al.* 1998). Recently, Fujimura et al. (2015) reported that the transfer factor of ^{137}Cs to rice was 0.011 – 0.031, which decreased with time. In our study site, more than 2% of deposited radionuclides can be enriched in wheat and maize when crops uptake nutrient from contamination soil based on the transfer factors of 0.009--0.021 and 0.005--0.041 (Gerzabek *et al.* 1998), and more than 4% of absorbed radionuclides can be entered the food chain without remediate measures after a nuclear accident.

The results showed that only < 4% of added ^{137}Cs and ^{60}Co migrated to 200–300 mm in both soils at 800th day. Moreover, no ^{137}Cs and ^{60}Co was detected in leachate samples indicating that ^{137}Cs and ^{60}Co did not infiltrate into the more than 200-300 mm soil depth during the study period. However, the migration rate of ^{137}Cs and ^{60}Co of the two test soils were 107–134 and 140–170 mm year^{-1}, respectively. Based on these migration rates, the ^{137}Cs and ^{60}Co released from nuclear accident may migrate into local groundwater (level 3 m) after several decades.

Therefore, emergency measures must be taken after a nuclear accident to protect human health and the environment. Removing the contaminated soil from highly confined contaminated areas after a nuclear accident immediately can effectively eliminate the impacts of these radionuclides on soil, water, and human health. In addition, combination of the chemical remediation (ion exchange method and oxidation–reduction method) and biological remediation (microbial remediation and phytoremediation) can be adopted under these circumstances at same time.

CONCLUSIONS

This study shows that ^{137}Cs and ^{60}Co deposited on farmland from simulated nuclear fallout remained within the plough layer (0–300 mm soil depth). After 800–days, between 80 to 89% of both radionuclides were present in the top 0–100 mm soil depth in Brown soil and Aeolian sandy soil; 9 to 16% migrated between 100–200 mm depth and only < 2% of ^{137}Cs and about 3% of ^{60}Co migrated to 200–300 mm depth in both soils. Some of these radionuclides may subsequently migrate into groundwater with high water table level after several decades. Among the soil properties studied, soil clay and silt fractions and SOC concentration, soil pH and solid-liquid distribution coefficient of the radionuclide (K_d) were the major influence factors affecting the migration of radionuclides in study area. Hence, to mitigate the impacts of deposited radionuclides on farmland soil surrounding nuclear power plant, agricultural management practices should be prohibited, and integrated measures must be taken urgently to protect human health and the environment.

ACKNOWLEDGEMENTS

We would like to thank the IAEA Project (Research Contract No. 18176) and the National Science and Technology Major Projects (2013ZX06002001) that supported this work. This work is part of the project supported by the National Key Research and Development Program of China (2017YFC0505402).

REFERENCES

Alvarez, R., Steinbach, H.S., 2009. A review of the effects of tillage systems on some soil physical properties, water content, nitrate availability and crops yield in the Argentine Pampas. Soil and Tillage Research 104, 1–15.

Blanco–Canqui, H., Wienhold, B.J., Jin, V.L., Schmer, M.R., Kibet, L.C., 2017. Long–term tillage impact on soil hydraulic properties. Soil and Tillage Research 170, 38–42.

Bossew, P., Gastberger, M., Gohla, H., Hofer, P., Hubmer, A., 2004. Vertical distribution of radionuclides in soil of a grassland site in Chernobyl exclusion zone. J. Environ. Radioact. 73, 87–99.

Bossew, P., Kirchner, G., 2004. Modelling the vertical distribution of radionuclides in soil. Part 1: the convection–dispersion equation revisited. J. Environ. Radioact. 73, 127–150.

Bunzl, K., Schimmack, W., Zelles, L., Albers, B.P., 2000. Spatial variability of the vertical migration of fallout ^{137}Cs in the soil of a pasture, and consequences for long–term predictions. Radiat Environ Biophys. 39, 197–205.

Chappell, A., 1998. Dispersing sandy soil for the measurement of particle size distributions using optical laser diffraction. Catena 31, 271-281.

Chibowski, S., Zygmunt, J., 2002. The influence of the sorptive properties of organic soils on the migration rate of ^{137}Cs. J. Environ. Radioact. 61, 213–223.

Cresswell, A.J., Kato, H., Onda, Y., Nanba, K., 2016. Evaluation of forest decontamination using radiometric measurements. J. Environ. Radioactiv. 164, 133–144.

Dowdall, M., Bondar, Y., Skipperud, L., Zabrotski, V., Pettersen, M.N., Selnæs, Ø.G., Brown, J.E., 2017. Investigation of the vertical distribution and speciation of ^{137}Cs in soil profiles at burnt and unburnt forest sites in the Belarusian Exclusion Zone. J. Environ. Radioact. 175–176, 60–69.

Dragovi, S., Gaji, B., Dragovi, R., Jankovi–Mandi, L., Slavkovi–Bekoski, L., Mihailovi, N., Momilovi, M., Uji, M., 2012. Edaphic factors affecting the vertical distribution of radionuclides in the different soil types of Belgrade, Serbia. Journal of Environmental Monitoring. 14, 127–137.

Dumat, C., Cheshier, M.V., Fraser, A.R., Shand, C.A., Staunton, S., 1997. The effect of removal of soil organic matter and iron on the adsorption of radiocaesium. Journal of Soil Science 48, 675–683.

Forkapic, S., Vasin, J., Bikit, I., Mrdja, D., Bikit, K., 2017. Correlations between soil characteristics and radioactivity content of Vojvodina soil. J. Environ. Radioact. 166, 104–111.

Fujimura, S., Muramatsu, Y., Ohno, T., Saitou, M., Suzuki, Y., Kobayashi, T., Yoshioka, K., Ueda, Y., 2015. Accumulation of ^{137}Cs by rice grown in four types of soil contaminated by the Fukushima Dai–ichi Nuclear Power Plant accident in 2011 and 2012. J. Environ. Radioact. 140, 59–64.

Gaspar, L., Navas, A., 2013. Vertical and lateral distributions of ^{137}Cs in cultivated and uncultivated soils on Mediterranean hillslopes. Geoderma. 207–208, 131–143.

Gerzabek, M.H., Strebl, F., Temmel, B., 1998. Plant uptake of radionuclides in lysimeter experiments. Environ. Pollut. 99, 93–103.

Guillén, J., Baeza, A., Corbacho, J.A., Muñoz–Muñoz, J.G., 2015. Migration of ^{137}Cs, ^{90}Sr, and $^{239+240}$Pu in Mediterranean forests: influence of bioavailability and association with organic acids in soil. J. Environ. Radioact.144, 96–102.

Gupta, D.K., Walther, C., 2014. Radionuclide contamination and remediation through plants. Springer, New York.

Hirose, K., 2016. Fukushima Daiichi Nuclear Plant accident: atmospheric and oceanic impacts over the five years. J. Environ. Radioact. 157, 113–130.

Hossain, M.A., Shamsuzzaman, M., Ghose, S., Hossain, A.K.M.A., 2012. Characterization of local soils and study the migration behavior of radionuclide from disposal site of LILW. J. Environ. Radioact. 105, 70–75.

IAEA, 2010. Handbook of parameter values for the prediction of radionuclide transfer in terrestrial. International Atomic Energy Agency, Vienna.

Jagercikova, M., Cornu, S., Le Bas, C., Evrard, O., 2015. Vertical distributions of ^{137}Cs in soils: a meta–analysis. J. Soil Sediment.15, 81–95.

Kamei–Ishikawa, N., Uchida, S., Tagami, K., 2008. Distribution coefficients for ^{85}Sr and ^{137}Cs in Japanese agricultural soils and their correlations with soil properties. J. Radioanal. Nucl. Chem. 277, 433–439.

Karadeniz, Ö., Karakurt, H., Çakır, R., Çoban, F., Büyükok, E., Akal, C., 2015. Persistence of ^{137}Cs in the litter layers of forest soil horizons of Mount IDA/Kazdagi, Turkey. J. Environ. Radioact. 139, 125–134.

Kato, H., Onda, Y., Teramage, M., 2012. Depth distribution of ^{137}Cs, ^{134}Cs, and ^{131}I in soil profile after Fukushima Dai–ichi Nuclear Power Plant Accident. J. Environ. Radioactiv. 111, 59–64.

Kirchner, G., Strebl, F., Bossew, P., Ehlken, S., Gerzabek, M.H., 2009. Vertical migration of radionuclides in undisturbed grassland soils. J. Environ. Radioact. 100, 716–720.

Koarashi, J., Atarashi–Andoh, M., Matsunaga, T., Sato, T., Nagao, S., Nagai, H., 2012. Factors affecting vertical distribution of Fukushima accident–derived radiocesium in soil under different land–use conditions. Sci. Total Environ. 431, 392–401.

Konoplev, A., Golosov, V., Wakiyama, Y., Takase, T., Yoschenko, V., 2017. Natural attenuation of Fukushima–derived radiocesium in soils due to its vertical and lateral migration. J. Environ. Radioact. 1–11.

Li, S.S., Wang, Z.M., Guo, Z.D., 2003. Study on migration of radionuclides in unsaturated loess. Atomic energy publishing house, Beijing. (in Chinese)

Li, Y., Geng, X.C., Yu, H.Q., Wan, G.J., 2011. Effects of the composition of standard reference material on the accuracy of determinations of 210Pb and 137Cs in soils with gamma spectrometry. Appl. Radiat. Isotopes. 69, 516–520.

Lepage, H., Laceby, J.P., Bonté, P., Joron, J., Onda, Y., Lefèvre, I., Ayrault, S., Evrard, O., 2016. Investigating the source of radiocesium contaminated sediment in two Fukushima coastal catchments with sediment tracing techniques. Anthropocene 13, 57–68.

López–Vicente, M., Onda, Y., Takahashi, J., Kato, H., Chayama, S., Hisadome, K., 2018. Radiocesium concentrations in soil and leaf after decontamination practices in a forest plantation highly polluted by the Fukushima accident. Environ. Pollut. 239, 448–456.

Mishra, S., Arae, H., Sorimachi, A., Hosoda, M., Tokonami, S., Ishikawa, T., Sahoo, S.K., 2015. Distribution and retention of Cs radioisotopes in soil affected by Fukushima nuclear plant accident. J. Soil Sediment. 15, 374–380.

Nakano, M., Yong, R.N., 2013. Overview of rehabilitation schemes for farmlands contaminated with radioactive cesium released from Fukushima power plant. Eng. Geol. 155, 87–93.

Navas, A., Soto, J., Machin, J., 2002. Edaphic and physiographic factors affecting the distribution of natural gamma–emitting radionuclides in the soils of the Arna's catchment in the Central Spanish Pyrenees. Eur. J. Soil Sci. 53, 629–638.

Pachepsky, Y., Park, Y., 2015. Saturated Hydraulic Conductivity of US Soils Grouped According to Textural Class and Bulk Density. Soil Sci. Soc. Am. J. 79, 1094.

Relyea, F. J., 1982. Theoretical and experimental considerations for the use of the column method for determining radionuclides retardation factors. Radioactive Waste Management and the Nuclear Fuel Cycle. 3:151–166.

Sahara, I., Sucharová, J., Holá, M., Pilátová, H., Rulík, P., 2016. Long–term retention of ^{137}Cs in three forest soil types with different soil properties. J. Environ. Radioact. 158–159, 102–113.

Salem, H.M., Valero, C., Muñoz, M.Á., Rodríguez, M.G., Silva, L.L., 2015. Short–term effects of four tillage practices on soil physical properties, soil water potential, and maize yield. Geoderma 237–238, 60–70.

Shakhashiro, A., Mabit, L., 2009. Results of an IAEA inter–comparison exercise to assess ^{137}Cs and total ^{210}Pb analytical performance in soil. Appl. Radiat. Isot. 67 (1), 139–146.

Shanthi, G., Thanka Kumaran, J.T., Gnana Raj, G.A., Maniyan, C.G., 2012. Transfer factor of the radionuclides in food crops from high–background radiation area of south west India. Radiat. Prot. Dosim. 149, 327–332.

Shinonaga, T., Schimmack, W., Gerzabek, M.H., 2005. Vertical migration of ^{60}Co, ^{137}Cs and ^{226}Ra in agricultural soils as observed in lysimeters under crop rotation. J. Environ. Radioactiv. 79, 93–106.

Shiozawa, S., 2012. Vertical Migration of Radiocesium Fallout in Soil in Fukushima. In: Nakanishi, T.M., Tanoi, K. (Eds.), Agricultural Implications of the Fukushima Nuclear Accident. Springer, pp. 49–60.

Šimanský, V., Juriga, M., Jonczak, J., Uzarowicz, Ł., Stępień, W., 2019. How relationships between soil organic matter parameters and soil structure characteristics are affected by the long–term fertilization of a sandy soil. Geoderma 342, 75–84. Soil Science Society of America, 2002. Methods of soil analysis, physical methods. In:Warren, A.D. (Ed.), Part 4, Madison, Wisconsin, USA.

Staunton, S., Dumat, C., Zsolnay, A., 2002. Possible role of organic matter in radiocaesium adsorption in soils. J. Environ. Radioact. 58, 163–173.

Takahashi, J., Tamura, K., Suda, T., Matsumura, R., Onda, Y., 2015. Vertical distribution and temporal changes of ^{137}Cs in soil profiles under various land uses after the Fukushima Dai–ichi Nuclear Power Plant accident. J. Environ. Radioact. 139, 351–361.

Teramage, M.T., Onda, Y., Kato, H., 2016. Small scale temporal distribution of radiocesium in undisturbed coniferous forest soil: Radiocesium depth distribution profiles. J. Environ. Manage. 170, 97–104.

Teramage, M.T., Onda, Y., Kato, H., Gomi, T., 2014. The role of litterfall in transferring Fukushima–derived radiocesium to a coniferous forest floor. Sci. Total Environ. 490, 435–439.

Teramage, M.T., Onda, Y., Kato, H., Wakiyama, Y., Mizugaki, S., Hiramatsu, S., 2013. The relationship of soil organic carbon to $^{210}Pb_{ex}$ and ^{137}Cs during surface soil erosion in a hillslope forested environment. Geoderma 192, 59–67.

Tsukada, H., Takeda, A., Hisamatsu, S., Inaba, J., 2008. Concentration and specific activity of fallout

^{137}Cs in extracted and particle–size fractions of cultivated soils. J. Environ. Radioact. 99, 875–881.

Tian, K., Zhao, Y., Xu, X., Hai, N., Huang, B., Deng, W., 2015. Effects of long–term fertilizatioand residue management on soil organic carbon changes in paddy soils of China: a meta–analysis. Agric. Ecosyst. Environ. 204, 40–50.

Page, A.L., Miller, R.H., Keeney, D.R. (Eds.), 1982. Methods of Soil Analyses, Part 2, Chemical and Microbiological Properties, 2nd ed. American Society of Agronomy, Madison, WI, USA, pp. 199–224.

Vahabi–Moghaddam, M., Khoshbinfar, S., 2012. Vertical migration of ^{137}Cs in the South Caspian soil. Radioprotection. 47, 561–573.

van der Graaf, E.R., Koomans, R.L., Limburg, J., de Vries, K., 2007. In situ radiometric mapping as a proxy of sediment contamination: Assessment of the underlying geochemical and –physical principles. Appl. Radiat. Isotopes. 65, 619–633.

Walther, C., Gupta, D.K., 2015. Radionuclides in the Environment. Springer, New York.

Wauters, J., Sweec, L., Valcke, E., Elsen, A., Cremers, A., 1994. Availability of radiocaesium in soils: a new methodology. The Science of the Total Environment 157, 239–248.

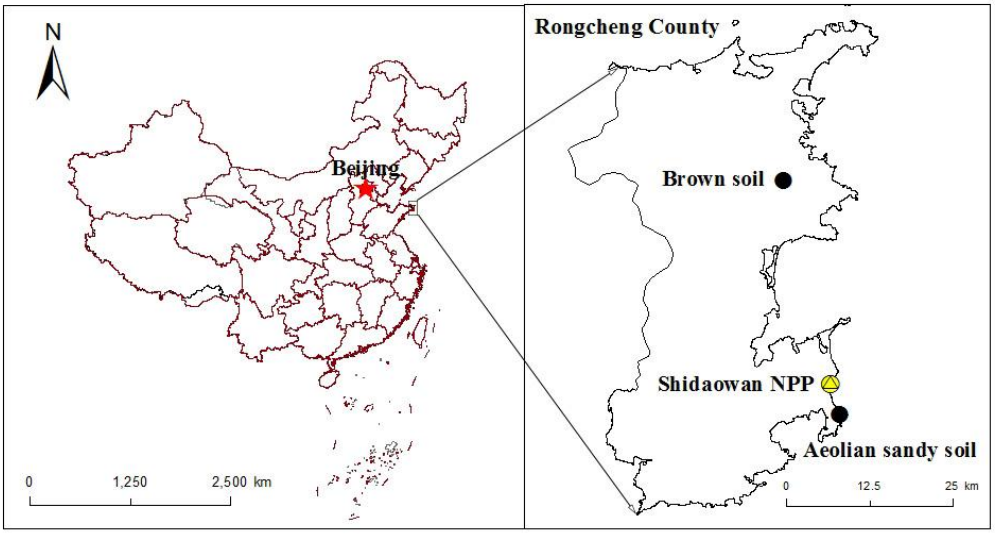

Fig.1. Location of study site (●sampling site).

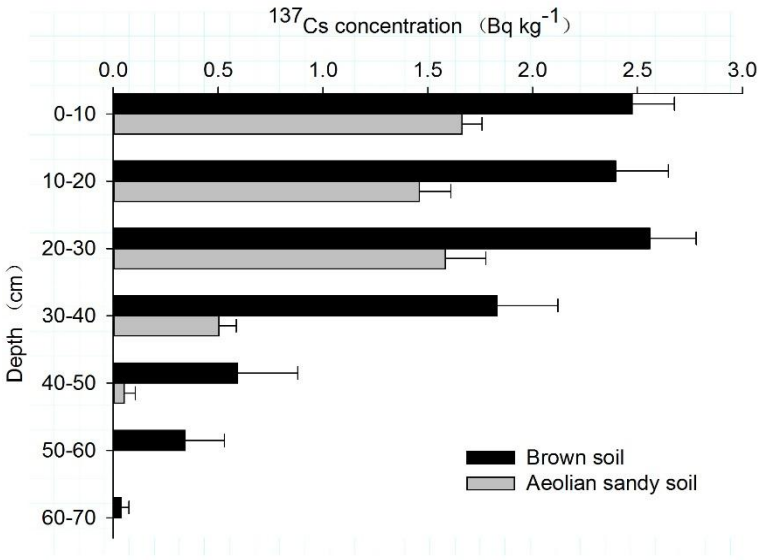

Fig.2. Background concentration of ^{137}Cs in Brown and Aeolian sandy soils. Each value represents the mean of three replicates ±standard error shown by horizontal bars.

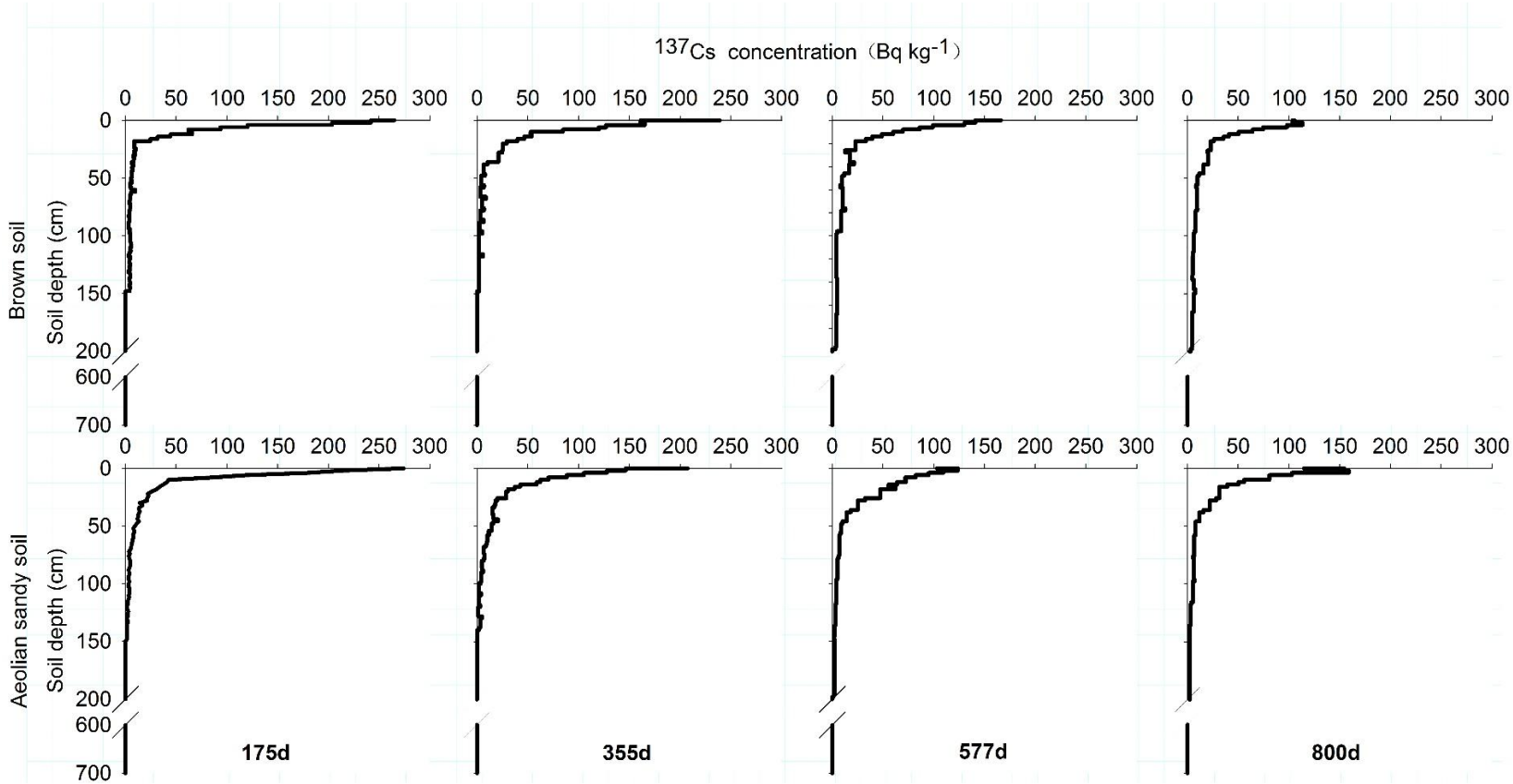

Fig.3. Dynamic migration of the added ^{137}Cs in soil profiles. Each value represents the mean of ^{137}Cs concentration in two undisturbed soil columns ± standard error shown by horizontal bars.

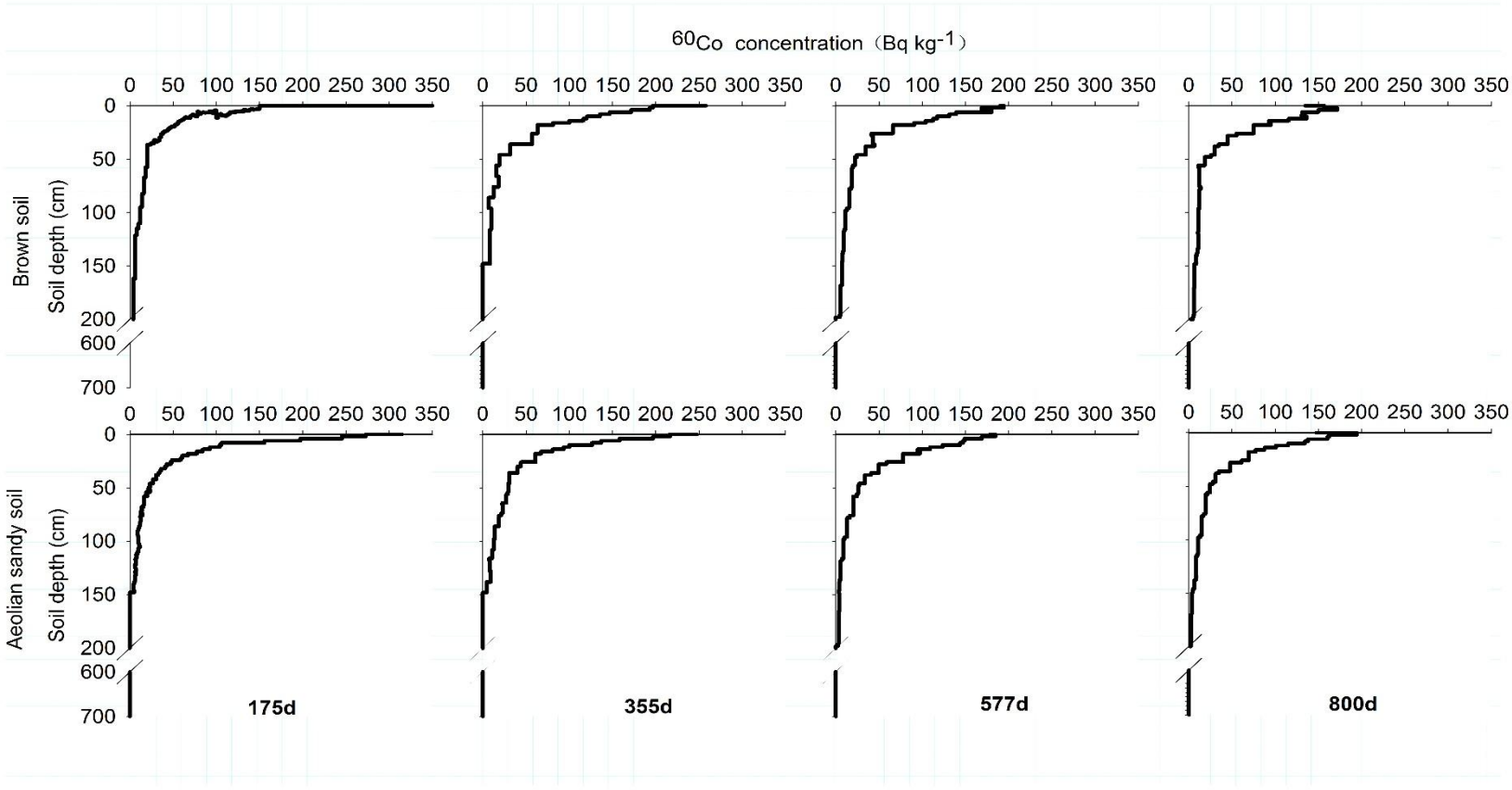

Fig.4. Dynamic migration of the added ^{60}Co in soil profiles. Each value represents the mean of ^{60}Co concentration in two undisturbed soil columns ± standard error shown by horizontal bars.

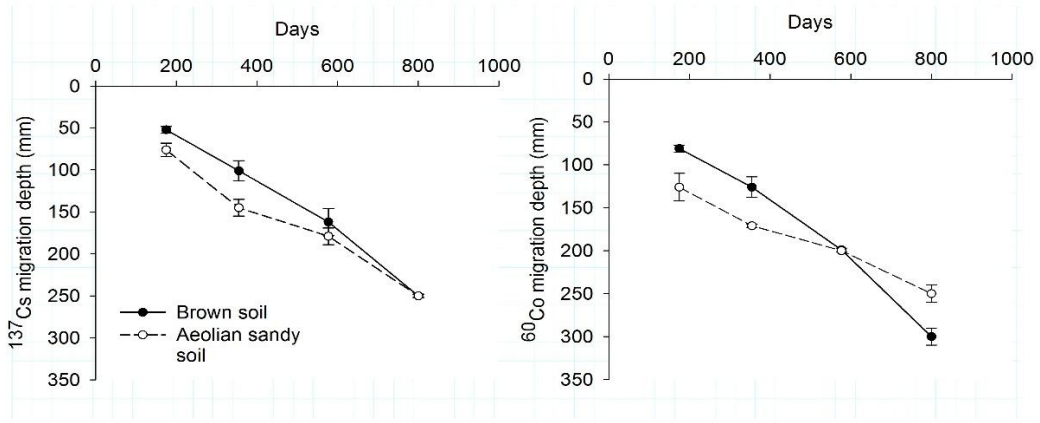

Fig. 5 Variation in migration depths of ^{137}Cs and ^{60}Co in Brown and Aeolian sandy soils during 800-day observation. Each value represents the mean of migration depth of ^{137}Cs and ^{60}Co in two undisturbed soil columns ± standard error shown by vertical bars.

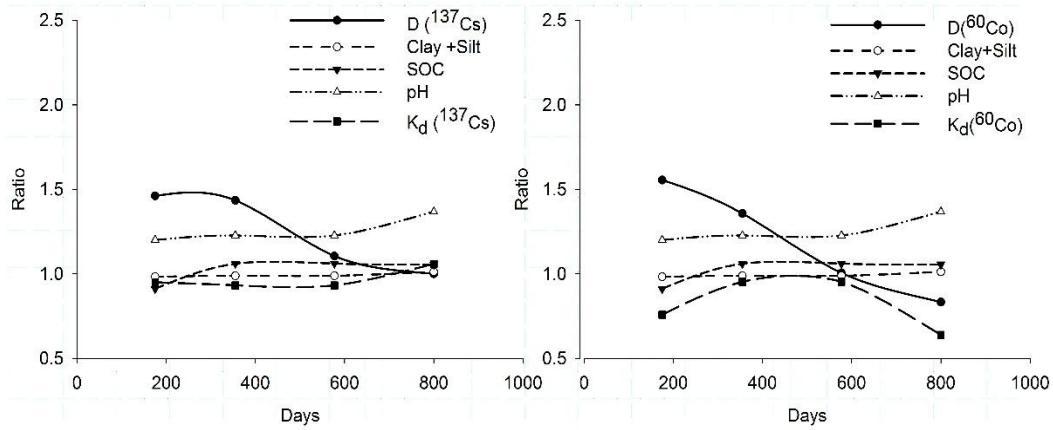

Fig. 6 The ratio of clay+silt fraction, SOC, pH, K_d, migration depth (D) of radionuclides (^{137}Cs and ^{60}Co) in Aeolian sandy soil to in Brown soil at each sampling time.